BUTTERWORTH HEINEMANN

*Polymer* Vol. 36 No. 13, pp. 2667–2670, 1995

0032-3861/95/$10.00 + 0.00

# Real-time *in situ* X-ray diffraction study of polyethylene deformation

**M. E. Vickers***
*BP Research and Engineering, Chertsey Road, Sunbury-on-Thames, TW16 7LN, UK*

**and H. Fischer†**
*University of Bristol, H. H. Wills Physics Laboratory, Tyndall Avenue, Bristol, BS8 1TL, UK*
*(Received 1 November 1994; revised 9 February 1995)*

A range of polyethylenes has been studied by X-ray diffraction during deformation. Changes in the crystalline orientation have been related to the load–extension curve. This was altered by changing the molecular weight, concentration of branches and strain rate. Crystalline orientation was first observed just after the maximum load, before any visible signs of yield. At about the same point, the monoclinic phase was observed in specimens that were subjected to a higher load and it disappeared when stress softening occurred. Initially the (110) orthorhombic reflection oriented to give four maxima, which implies tilted polymer chains and lamellae. Subsequently the (110) concentrated on the equator showing chains oriented parallel to the draw direction. The transition from tilted to fibre orientation occurred at different points on a nominal stress–strain curve but at approximately the same local strain, as estimated from the change in sample dimensions.

**(Keywords: deformation; polyethylene; X-ray scattering)**

## *Introduction*

The deformation of polyethylene is a complex process and it has been extensively studied[1–3]. The unoriented original spherulitic structure, which contains regions of lamellae stacked in every direction, is deformed and eventually destroyed to give a fibrillar structure with the polymer chains oriented in the draw direction. Early work was on homogeneous samples[4,5] and subsequently studies were made on specially prepared samples to confirm particular mechanisms[1,2,6]. The lamellae have been reported to separate, tilt, untwist, and to undergo interlamellar slip, and fine and coarse intralamellar slip. The crystalline regions may undergo twinning, a phase change, slip and become strained[7] and the non-crystalline regions can become oriented and strained. Most studies have not related structural changes to the stress–strain curve. Only a few real-time *in situ* studies have been carried out[8–13] and, with two exceptions[12,13], they were performed at elevated temperature. In general, these results are consistent with the mechanisms proposed from *ex situ* work.

It is well established that both the modulus and yield strength tend to increase with increasing density[2,14]. The yield has generally been related to lamellar thickness[14–17], while the modulus has been related to lamellar thickness[14] or the reduced amount of non-crystalline material and/or tie-molecules[14] (molecules that bridge two or more crystalline lamellae), or to an increase in the amorphous modulus caused by thicker lamellae[16]. Recent work has confirmed the existence of double yield points[18–20], the first predominantly recoverable and the second associated with necking and irrecoverable.

This work was undertaken in an attempt to provide more basic understanding of the structural changes that occur at particular points on the stress–strain curve.

## *Experimental*

Small dumb-bells (*Table 1*) were cut from pressed plaques of the materials described in *Table 2* and marked with a millimetre scale. The specimens were deformed in a Minimat small-scale tensile tester with software control. It was observed that most of the specimens yielded at a similar position (about 4 mm from the fixed end) and the neck propagated towards the moving end. The rig was positioned so that the X-ray beam (1 $mm^2$) illuminated this position, and specimens were observed during deformation to check that they did yield at the expected position. Most runs were carried out at a crosshead speed of 1 mm $min^{-1}$ ($2.78 \times 10^{-3}$ $s^{-1}$) but some fast runs (10 mm $min^{-1}$) and a few slow ones (0.1 mm $min^{-1}$) were also performed.

The X-ray data were collected in transmission with CuK$\alpha$ radiation, a Siemens two-dimensional electronic detector and a sample-to-detector distance of 35 mm, which gave a range of 5–45° 2$\theta$. Most of the data were collected in 10 s frames with 17 s between frames. The fastest data collections were 3 s frames with 3.5 s for data dumping, and some longer data collections were carried out to obtain information on the weaker reflections. A few relaxation measurements were made *in situ*. The air scattering, collected with no sample, was subtracted from the data, but other corrections for detector response and spatial aberations were found to be negligible and hence not applied. In addition, to confirm and extend the *in situ* work, some *ex situ* studies were carried out using standard wide- and small-angle X-ray scattering (WAXS and SAXS) photographic techniques and a four-circle diffractometer. The minimum time from unloading the sample to completion of an azimuthal scan was 5 min

* To whom correspondence should be addressed. Present address: Department of Materials Science and Metallurgy, University of Cambridge, CB2 3QZ, UK
† Present address: Department of Polymer Technology, University of Eindhoven, Eindhoven, The Netherlands

(1.5 min scans) but the time for SAXS data was about 30 h.

Because most of the polymers necked in a localized region ($\sim 1\ mm^2$), the extensions were not converted to nominal strain. To obtain an estimate of the local strain at which the transition from tilted to fibre orientation occurred, the width and thickness of the specimens were measured and any changes in volume were assumed to be negligible. This approach is likely to somewhat underestimate the local strain, particularly for the highest molecular weight polymer E, which gave the greatest relaxation on unloading[21].

**Table 1** Dumb-bell dimensions (mm)

| | |
|---|---|
| Gauge length | 6 |
| Gauge width | 3 |
| Thickness | 0.2–0.3 |
| Total length | 25 |
| Radius | 2 |
| Maximum width | 8 |

**Table 2** Description of materials

| Material[a] | $M_w$ | Butyl branches/000 C atoms |
|---|---|---|
| A | 131 000 | <0.5 |
| B | 206 000 | 6.2 |
| C | 126 000 | 21 |
| D | 385 000 | <0.5 |
| E | $\sim 1.5 \times 10^6$ | <0.5 |

[a] Materials A–C were studied by Brooks *et al.*[18]

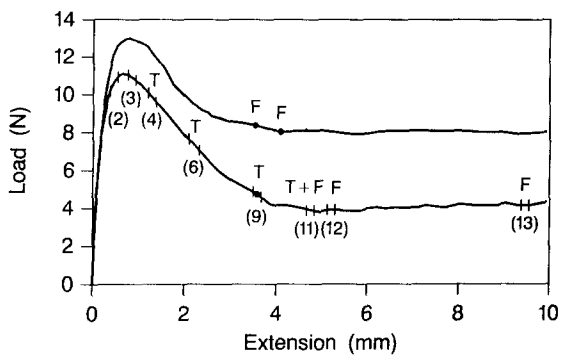


**Figure 1** Load *versus* extension for polymer A (lower curve standard and upper curve fast strain rates) showing transition from tilted to oriented fibre morphology: ||, *in situ* data (frame number); ●, *ex situ* data; T, tilted; F, fibre orientation

*Results and discussion*

*Figure 1* shows the load–extension curve for polymer A and the intervals within which X-ray data were collected. *Figure 2* gives the corresponding two-dimensional WAXS data and *Figure 3* shows azimuthal scans around the (110) reflection. The slight shadow in the background scattering was probably from the sample or the rig. Initially the sample was unoriented. Evidence for crystalline orientation near the first yield point was inconclusive. There was probably just a very small amount of crystalline orientation. Frames 4 to 6 showed increasing crystalline orientation with (110) maxima at about 40, 150, 210 and 330° from the equator, described as tilted orientation. In these frames an additional peak appeared inside the (110), which is considered to be the (001) reflection of monoclinic polyethylene. In frames 8 and 9 the (001) monoclinic peak became oriented and (110) maxima moved closer together. By frame 11 there were probably equatorial (110) maxima, implying coexistence of tilted and fibre orientation. The fibre orientation in frame 12 became sharper in frame 13 and the monoclinic phase disappeared. No tilting was observed for the (200) orthorhombic reflection; it oriented gradually on the equator, consistent with *ex situ* studies on cold drawing[4]. With hot drawing, the (200) reflection has been reported to tilt and have an equatorial population[8,9].

*Figure 4* summarizes the results on all five polymers. The shape of the deformation curve was observed to be

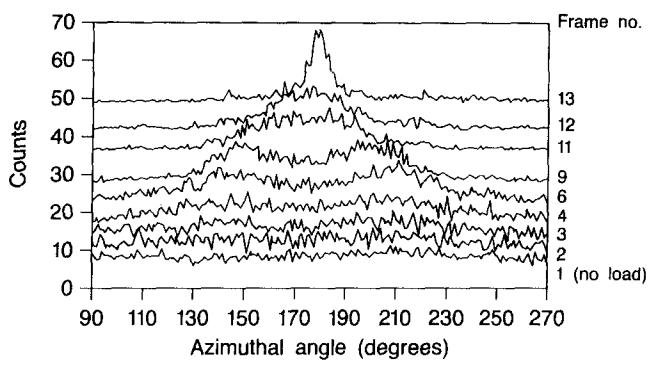


**Figure 3** *In situ* WAXS data on polymer A (standard strain rate). Azimuthal scan on (110) reflection

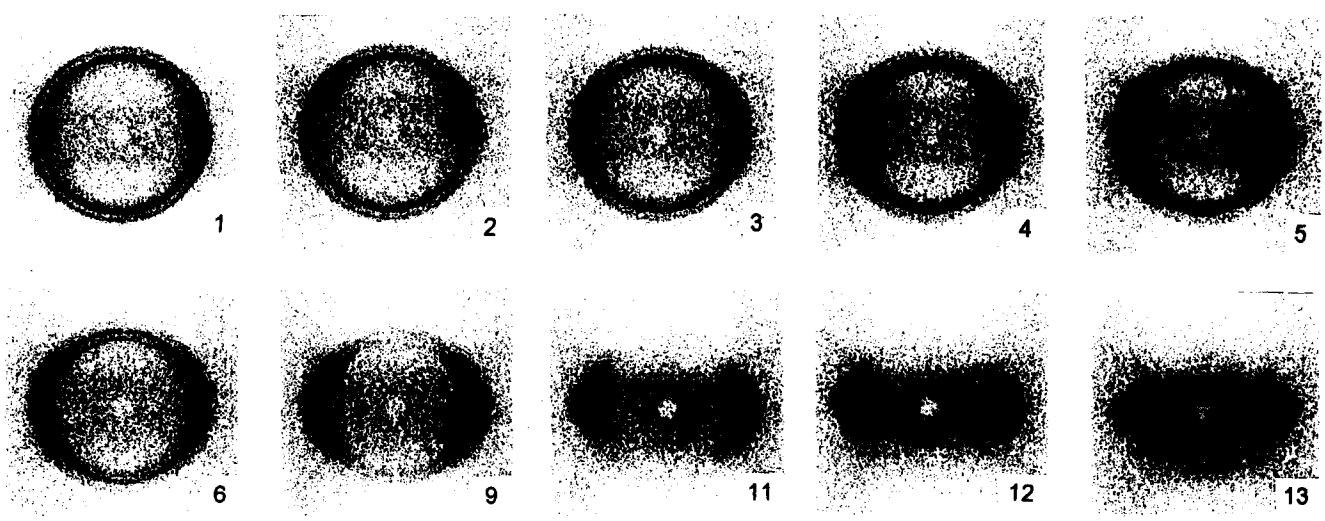


**Figure 2** *In situ* WAXS data on polymer A (standard strain rate), draw direction vertical. Frame 1, 30 s; frames 2–6, 9 and 11–13, 10 s

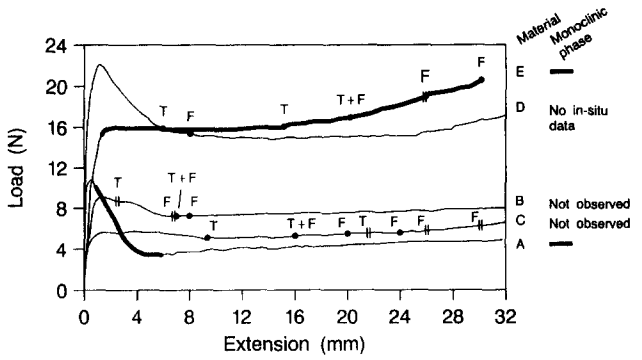


**Figure 4** Load *versus* extension for polymers A, B, C, D and E (standard strain rate), showing transition from tilted to oriented fibre morphology and presence of monoclinic phase: ‖, *in situ* data; ●, *ex situ* data; T, tilted; F, fibre orientation

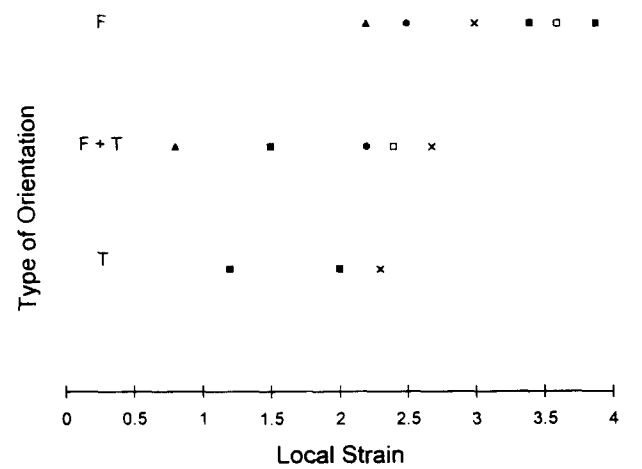


**Figure 5** Type of crystalline orientation *versus* local strain: ■, A; □, B; ×, C; ●, D; ▲, E; T, tilted; F, fibre orientation

sensitive to changes in the molecular structure of PE, as reported in the literature[14,21]. At the position of maximum load (about 1 mm extension), no local strain nor whitening was observed. Polymers A and D whitened at extensions of about 1.8 and 2.8 mm, respectively, and polymers A, B, C and D necked at 3, 4.5, 8.5 and 4 mm, respectively. No inhomogeneous deformation was observed for polymer E.

Tilted crystalline orientation was observed in all the samples before any visible signs of yield, and the sequence of changes from no orientation to tilted to fibre orientation was similar for all the materials. The major difference was the extension at which the transition from tilted to fibre orientation was complete. Thus the transition from tilted to fibre orientation can be related to the deformation curve. Materials with a higher molecular weight or more side-chains maintained the tilted morphology for longer. For these materials the deformation was spread over a larger region of the sample. The data in *Figure 5* imply that the transition from tilted to fibre orientation occurred at approximately the same local strain (2–3.5), which is not dissimilar from the value reported for the transition in shear (4.3)[22]. The transition also occurred at a lower extension for faster deformation rates (but approximately the same local strain), consistent with the changes in the deformation curve.

Some relaxation studies were carried out to check the validity of *ex situ* data, extend the range of *in situ* data and to investigate the relaxation process itself. No relaxation in the crystalline orientation was observed *in situ* after 5 min with or without load near the first and second yield points. However, relaxation was noted after more than 15 min. The crystalline orientation at the first yield point was too weak to study. *Figure 6* shows *ex situ* (110) azimuthal scans on B after extension to 3 mm, just before the second yield point. Changes in both the peak intensity and position imply that the amount of oriented crystalline material and the angle of the oriented crystalline chains relative to the fibre axis decrease and reach a plateau after about 8 h. As expected, after larger extensions the relaxation was slower and a higher proportion of material remained oriented, consistent with Bartczak *et al.*[22,23].

The monoclinic phase was only observed in materials A and E, which were subjected to a higher load. At higher extensions, loss of the monoclinic phase in lower molecular weight samples and its retention in higher molecular weight material is consistent with Steidl and Pelzbauer[21]. The monoclinic phase has been observed in material C when thicker samples (1 mm) were deformed[12], and it is expected that all these materials might undergo this phase transformation under suitable conditions. The data suggest that when the monoclinic phase first appeared its orientation lagged behind that of the orthorhombic phase, but subsequently both phases became highly oriented.

*Ex situ* diffractometer azimuthal scans on the (200), (020) and (002) reflections confirmed that, for samples with the tilted orientation, the *a* axis was always perpendicular to the draw direction, with the *b* axis about 60° and the *c* axis about 30° from the draw direction. Data parallel and perpendicular to the plane of the sample were similar, consistent with the expected cylindrical symmetry. For sample E, drawn to 15 mm, in addition to the peak at about 30° there was a diffuse (002) maximum around 0°, in the draw direction. The *ex situ* SAXS data, on similar samples, gave a weak four-point pattern with the spots tending to streaks. This confirms that the lamellae were tilted and probably beginning to break up. The polymer chains were approximately perpendicular to the lamellar face in all the samples that were examined. However, most samples gave very poor SAXS data, probably owing to relaxation occurring during the time required for data collection and/or destruction of the lamellar repeat.

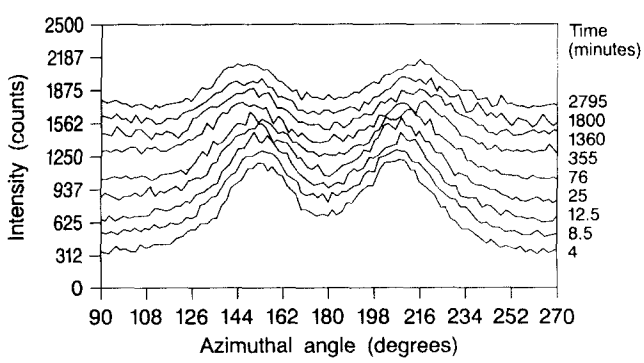


**Figure 6** Relaxation of polymer B after extension of 3 mm; azimuthal scan on (110) reflection at time from cessation of drawing

This preliminary study does not provide conclusive evidence for which particular mechanisms are responsible for the first and which for the second yield point. Interpretation is limited by the quality of the data. Further work on thicker samples, probably using a synchrotron source, with *in situ* SAXS and the yield points more clearly separated, is required. Information on amorphous regions would also be informative.

## *Conclusions*

This work shows that there is no observable crystalline orientation before the first yield point; tilted crystalline orientation starts at or just after the first yield and before any visible sign of yielding. The transition from tilted to fibre orientation occurs at approximately the same local strain, although the nominal strain increases with increasing molecular weight and concentration of branches. The results are consistent with the first yield point being predominantly reversible and the second one irreversible and associated with destruction of lamellae.

## *Acknowledgements*

We would like to thank BP Chemicals for permission to publish this paper and many BP Chemicals colleagues for their help and contributions. BP would like to thank Professor E. Atkins (University of Bristol) for permission to use the *in situ* X-ray facility.

## *References*

1 Lin, L. and Argon, A. S. *J. Mater. Sci.* 1994, **29**, 294
2 Bowden, P. B. and Young, R. J. *J. Mater. Sci.* 1974, **9**, 2034
3 Peterlin, A. *J. Mater. Sci.* 1971, **6**, 490
4 Kasai, N. and Kakudo, M. *J. Polym. Sci.* 1964, **A2**, 1955
5 Hay, I. L. and Keller, A. *Kolloid Z. Z. Polym.* 1965, **204**, 43
6 Pope, D. P. and Keller, A. *J. Polym. Sci. Phys.* 1975, **13**, 533
7 Dixon, N. M., Chai, C., Gerrard, D. L. and Reed, W. European Symposium on Polymer Spectroscopy, Vallaldoild, Spain, 1994
8 van Aerle, N. A. J. and Braam, A. W. M. *Colloid Polym. Sci.* 1989, **267**, 323
9 van Aerle, N. A. J. and Braam, A. W. M. *Makromol. Chem.* 1988, **189**, 1568
10 Wilke, W. and Bratrich, M. *J. Appl. Cryst.* 1991, **25**, 645
11 Dupius, J., Legrand, P., Seguela, R. and Rietsch, F. *Polymer* 1988, **29**, 626
12 Butler, M. F., Ryan, A. J., Bras, W. and Donald, A. M. *Macromolecules* (submitted)
13 Holland-Moritz, K., Stach, W. and Holland-Moritz, I. *Prog. Colloid Polym. Sci.* 1980, **67**, 161
14 Popli, R. and Mandelkern, L. *J. Polym. Sci. (Phys.)* 1987, **25**, 441
15 Young, R. J. *Mater. Forum* 1988, **11**, 210
16 Crist, B., Fisher, C. J. and Howard, P. R. *Macromolecules* 1989, **22**, 1709
17 Darras, O. and Seguela, R. *J. Polym. Sci. (Phys.)* 1993, **31**, 759
18 Brooks, N. W., Duckett, R. A. and Ward, I. M. *Polymer* 1992, **33**, 1872
19 Seguela, R. and Rietsch, F. *J. Mater. Sci. Lett.* 1990, **9**, 46
20 Springer, H., Hengse, A. and Hinrichsen, G. *Colloid Polym. Sci.* 1993, **271**, 523
21 Steidl, J. and Pelzbauer, Z. *J. Polym. Sci. Part C* 1972, **38**, 345
22 Bartczak, Z., Argon, A. S. and Cohen, R. E. *Polymer* 1994, **35**, 3427
23 Bartczak, Z., Cohen, R. E. and Argon, A. S. *Macromolecules* 1992, **25**, 4692